

PACS numbers: 42.30.Ms; 87.64.Cc; 87.63.–L
DOI: 10.1070/QE2013v043n07ABEH014953

Visualisation of blood and lymphatic vessels with increasing exposure time of the detector

V.V. Kalchenko, Yu.L. Kuznetsov, I.V. Meglinski

Abstract. **We describe the laser speckle contrast method for simultaneous noninvasive imaging of blood and lymphatic vessels of living organisms, based on increasing detector exposure time. In contrast to standard methods of fluorescent angiography, this technique of vascular bed imaging and lymphatic and blood vessel demarcation does not employ toxic fluorescent markers. The method is particularly promising with respect to the physiology of the cardiovascular system under *in vivo* conditions.**

Keywords: *speckle contrast, exposure time, 'white' vessels, blood vessels, lymphatic vessels.*

1. Introduction

The development of noninvasive imaging methods and quantification of microcirculatory blood and lymph flow *in vivo* has been of special interest for last several decades in the problems of optical diagnostics [1–5]. The concept of microcirculation combines a number of physiological processes occurring in the peripheral vascular bed of the circulatory and lymphatic systems as well as in the intercellular space of the body [6–12]. Variations in the values of microcirculatory blood and lymph flow may be an indicator of a variety of pathological processes that are closely associated with various diseases, including diabetes [13], atherosclerosis [14], varicose veins [15], anaemia [16], coronary artery disease [17], etc.

The lymphatic system plays a key role in the human body and works in conjunction with the system of blood vessels, ensuring normal circulation of interstitial fluid. The lymphatic system is an integral part of tissue fluid homeostasis, fat absorption in the small intestine and the immune response to a variety of pathological conditions including inflammation, lymphedema and tumour metastasis. Lymph itself is a liquid consisting of macromolecules, leucocytes and activated antigen-presented cells that move from blind-ended lymph capillaries to collecting lymph vessels and return to the bloodstream via the lymph ducts [6, 12].

V.V. Kalchenko, Yu.L. Kuznetsov Department of Veterinary Resources, Weizmann Institute of Science, Rehovot, 76100, Israel; e-mail: a.kalchenko@weizmann.ac.il, yuri.kuznetsov@weizmann.ac.il;
I.V. Meglinski Department of Physics, University of Otago, PO Box 56, Dunedin 9054, New Zealand; Research-Educational Institute of Optics and Biophotonics, N.G. Chernyshevsky Saratov State University, ul. Astrakhanskaya 83, 410012 Saratov, Russia; e-mail: igor.meglinski@otago.ac.nz

Received 6 August 2012; revision received 4 December 2012
Kvantovaya Elektronika **43** (7) 679–682 (2013)
Translated by I.A. Ulitkin

Today, there are quite a number of methods that are specially designed for the visualisation of the vascular bed and actively used in clinical practice, including X-rays and computed tomography [17], magnetic resonance imaging [18], ultrasonic method using the Doppler effect [19], laser Doppler flowmetry (LDF) [5], scanning confocal microscopy [20], optical coherence tomography (OCT) [21, 22], capillaroscopy [23], fluorescence intravital microscopy (FIM) [24], etc. Despite significant progress in the development of methods of cardiovascular system diagnostics, final understanding of the functioning of the lymphatic system, however, is still incomplete due to lack of suitable methods for noninvasive imaging of lymph flow and lymph microstructures under *in vivo* conditions.

The ultrasonic method relying on the Doppler effect provides the required resolution for the measurement of blood flow velocity in blood vessels of different tissues, but the acoustic wavelength, required for penetration into deep tissues, is limited by spatial resolution down to 200 μm. Using capillaroscopy requires tissues to be sufficiently thin (less than 400 μm). Magnetic resonance angiography provides information mainly about large blood vessels, such as coronary arteries. Disadvantages of the OCT are high sensitivity to involuntary movements of the object under study and impossibility of measurement of the flow parameters in lymph and blood vessels less than 50 μm in diameter at a flow velocity less than 100 μm s^{-1}. Strong optical scattering of probe laser radiation in biological tissues severely limits the spatial resolution in measuring the velocity of the blood flow by LDF.

Lymph vessels and lymph nodes connected together in a complex network in which lymph moves toward the heart are traditionally visualised by FIM using fluorescent contrast agent injection [24–26]. Despite the quality of the images and high resolution, this method depends essentially on biochemical characteristics and toxicity of the administered fluorescent substance, thus limiting its applicability.

In the present work we present the laser speckle contrast (LSC) technique of simultaneous noninvasive imaging of blood and lymphatic vessels of living organisms with increasing exposure time of the detector. LSC imaging is based on the principles of dynamic light scattering (DLS) [27]. Many variations of the DLS method worked well in a variety of biomedical applications of diagnostic nature, such as control of changes in the capillary blood flow [28], imaging of blood coagulation [29], mapping of blood perfusion [30], etc. In connection with problems of percutaneous visualisation of the blood flow and measurement of perfusion, LSC is an alternative to LDF [5], diffusion-wave spectroscopy [31–34] or diffusion LDF [35]. When using LCS, imaging of the vas-

cular bed and the demarcation of lymphatic and blood vessels are carried out without the use of fluorescent markers, which removes restrictions on the applicability of the method associated with toxicity.

2. Experimental

Figure 1 shows a schematic diagram of the experimental setup used in this paper to visualise blood and lymphatic vessels *in vivo*. The setup combines the possibility of simultaneous and alternating application of FIM and LSC [24–26]. In the FIM regime, as a light source use is made of a mercury lamp, light from which passes through the optical filter F1 (460–490 nm) and is projected by a dichroic mirror DM onto the object under study (in our case a mouse ear under anaesthesia). The fluorescent signal is detected with a CCD-camera (Pixelfly QE, PCO, Germany) in the spectral range of 510–550 nm (filter F2).

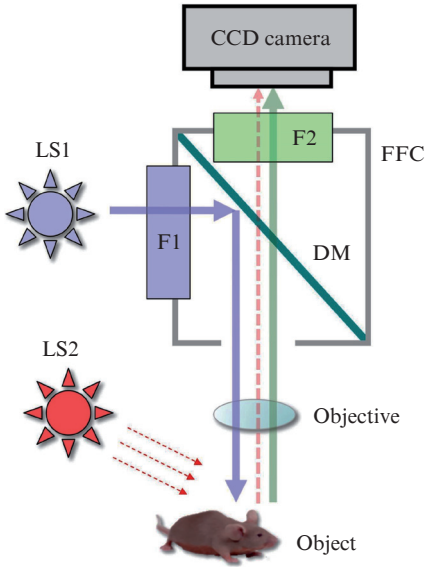

Figure 1. Scheme of the LSC-FIM bimodal experimental setup for imaging the vascular bed and microcirculatory blood and lymph flow *in vivo*: (LS1) and (FFC) mercury discharge lamp and fluorescent filtration cube, which are part of a standard fluorescent illuminator of a SZX 12 RFL2 stereomicroscope (Olympus, Japan); (LS2) 10-mW, 670-nm scattered coherent laser light source (ELFI-C, Israel).

In the LSC regime, the laser (Roithner Lasertechnik, Austria; wavelength of 808 nm, output power of 10 mW) diffusely illuminates the same region of the mouse ear. Due to the movement of light scattering blood cells such as erythrocytes and lymphocytes, the intensity of the detected backscattered laser light fluctuates to form a time-varying speckle pattern. The intensity of the speckle pattern $I(x,y)$ is recorded sequentially in equal time intervals, T, determined by the exposure time of the CCD camera (see Fig. 1). The resulting video sequence of N frames is divided into groups of n images each (in this case, $N = 300$ and $n = 10$), followed by calculation of the time-averaged speckle contrast

$$K(x,y) = \frac{1}{\gamma}\sum\frac{\sigma(x,y)}{\langle I(x,y)\rangle_n}. \quad (1)$$

Here, σ is the standard deviation, and $\langle I\rangle$ is the mean intensity at a given point (x,y) (pixel) of the speckle pattern $I(x,y)$; $\langle\ldots\rangle_n$ means averaging over a sample of n images of the video sequence; and $\gamma = N/n$. The process of detecting the video sequence and the calculation of the time-averaged speckle contrast $K(x,y)$ are fully automated by means of a specially developed software, created on the basis of ImageJ built-in editor (NIH, USA) with the possibility of further analysis, statistic and colour processing of the images obtained. The CCD camera was controlled using CamWare software (PCO, Germany).

All experimental procedures were carried out in full accordance with international standards for laboratory animal welfare and in accordance with the internal ethical standards of the Weizmann Institute. Laboratory animal anaesthesia was performed by intraperitoneal injection of a mixture of 10 mg of ketamine (Fort Dodge, Iowa, USA) and 100 mg of xelazine (Kepro, Deventer, The Netherlands) per 1 kg of body weight for a CD1 Nude female mouse at the age of 6–8 weeks, taken from Harlan Laboratories (Rehovot, Israel). The animal was kept in thermal comfort.

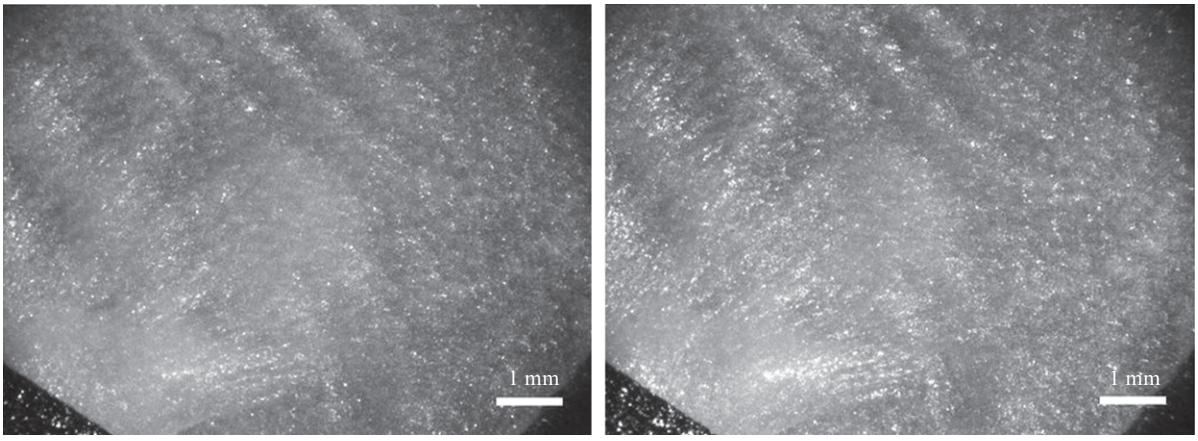

a b

Figure 2. Typical images of speckle patterns $I(x,y)$, observed on the surface of the mouse ear *in vivo*, at (a) short ($T = 33$ ms) and (b) long ($T = 650$ ms) exposure times of the CCD camera.

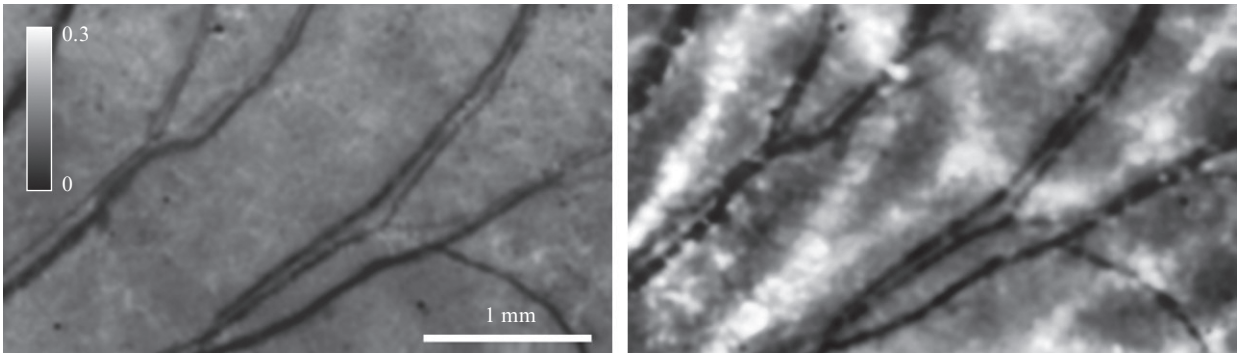

Figure 3. Fragment of speckle contrast images, $K(x,y)$ after averaging speckle patterns $I(x,y)$, observed in the outer surface of the mouse ear, at (a) short ($T = 33$ ms) and (b) long ($T = 650$ ms) exposure times of the detector.

3. Results and discussion

Figure 2 shows an image of a typical speckle pattern $I(x,y)$ received by the CCD camera from the surface of the mouse ear *in vivo*. The resulting speckle contrast images, $K(x,y)$, at a short (33 ms) and long (650 ms) exposure time T of the detector are presented in Fig. 3. In the case of a longer exposure time one can clearly see 'white' vessels in the image (Fig. 3b). This fact is explained by changes in sensitivity of the LCS method, determined in accordance with [36] as

$$S = \tau_c \frac{r}{2K}\left[\frac{1}{2r^2} - \frac{2r+1}{2r^2}\exp(-2r)\right], \quad (2)$$

where $r = T/\tau_c$ is the ratio of the detector exposure time T to the correlation time of intensity fluctuations of scattered laser light, τ_c, which is determined by the characteristic time of the spatial displacement of blood cells (erythrocytes and lymphocytes) by a distance of the order of the probe wavelength λ and is inversely proportional to the average speed $\langle v\rangle$ of movement of the latter ($\tau_c \sim \lambda/\langle v\rangle$). The speckle contrast K according to [36] is also a function of exposure time of the detector, T, and the correlation time, τ_c, and with acceptable accuracy may be represented as

$$K = \left\{\frac{\tau_c}{2T}\left[1 - \exp\left(-\frac{2T}{\tau_c}\right)\right]\right\}^{1/2}. \quad (3)$$

Figure 4a shows the sensitivity of the LSC method as a function of the exposure time of the detector, $S(T)$. One can easily see that the maximum sensitivity is obtained when the exposure time is comparable to the detector correlation time ($T \sim \tau_c$), whereas at $T \gg \tau_c$ and $T \ll \tau_c$ the sensitivity is minimal ($S \to 0$).

Figure 4b illustrates the sensitivity of the method as a function of correlation time $S(\tau_c)$ at a fixed exposure time of the detector used in the experiment ($T = 33$ and 650 ms). One can see that in the case of a prolonged exposure time of the detector ($T = 650$ ms), the sensitivity S for the correlation time $\tau_c \sim 10^2$ ms or longer increases substantially. Note that the range $\tau_c > 10^2$ ms corresponds to an extremely slow movement of the scattering particles whose speed is comparable to the speed of movement of the lymph flow.

To confirm or refute this fact/assumption, we used the FIM method [24–26], specifically designed for direct visualisation of lymphatic vessels. Figure 5 shows the image of the

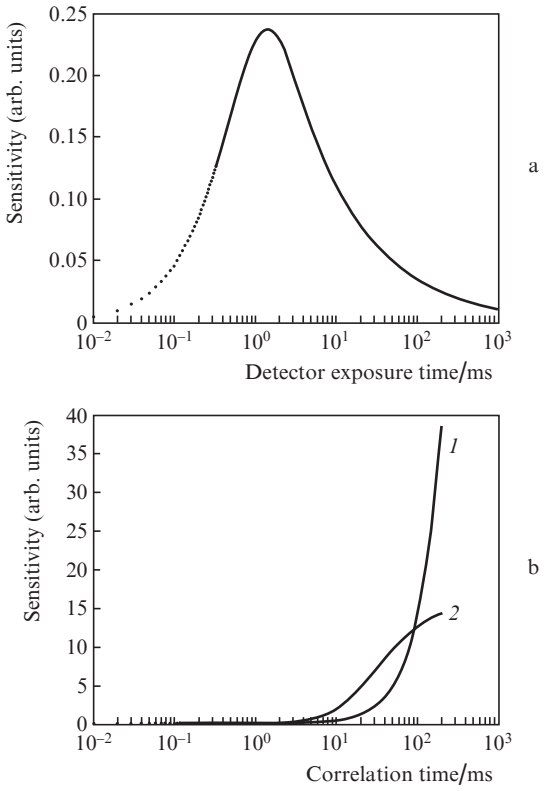

Figure 4. Sensitivity of the LCS method as a function of (a) the detector exposure time T and (b) the correlation time τ_c at the detector exposure times (*1*) 650 and (*2*) 33 ms.

vascular bed of the outer ear of the mouse in vivo, obtained by the LSC method, with superimposed contours of the lymphatic vessels obtained by FIM. Visualisation of lymphatic vessels in the FIM regime preceded intradermal injection of 2 μL of FITC dextran at a concentration of 10 mg mL^{-1} in the mouse ear. The visible pattern of lymphatic vessels, resulting from FIM, does not always repeat the profile of 'white' vessels, obtained by the LSC method. In our opinion, this is explained by the complex time-dependent, spatially inhomogeneous character of the lymph flow. The lymph flow in lymphatic vessels is usually of oscillatory nature with the pulsation frequency varying in the range of 1–11 min^{-1} [37]. In the case of low irradiation intensities and frequency of lymph flow pulsations, not all lymphatic vessels can be visualised by the

LSC method. Furthermore, not always the fluorescent contrast agent concentration at the site of a single vessel is sufficient to excite the fluorescent signal that can overcome the FIM sensitivity threshold. However, the results of the experiments presented here (see Fig. 5) suggest that the contours of the lymphatic vessels observed by the LSC method in the case of a sufficiently long exposure time of the detector and obtained by direct FIM measurements are in good agreement and repeat each other.

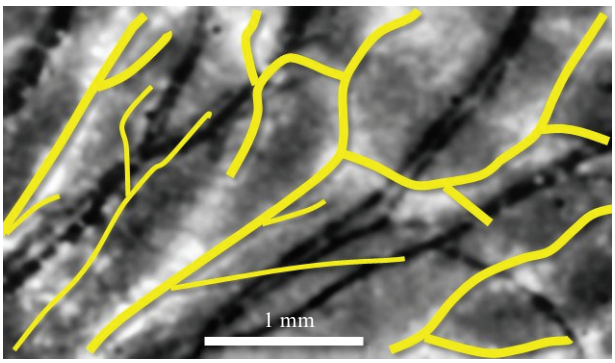

Figure 5. Fragment of the image of the vascular bed of the mouse's outer ear obtained by the LCS method in the case of a long ($T = 650$ ms) detector exposure time (see Fig. 2b) with superimposed contours of lymphatic vessels reproduced by FIM [24–26].

4. Conclusions

Thus, this study shows that in case of a longer exposure time of the detector, the LSC method allows simultaneous visualisation of not only blood, but also lymphatic vessels. This technique of simultaneous imaging of lymphatic and blood vessels, and their demarcation carried out without the use of toxic fluorescent markers, appears to be very promising in the applications to the physiology of the cardiovascular system, including the study of the lymphatic system.

Acknowledgements. This work was supported by Bernard Jaffe Foundation, internal staff scientists grant programme of the Weizmann Institute of Science (Israel) and was partially supported by the Royal Society of New Zealand.

References

1. Tuchin V.V. *Opticheskaya biomeditsinskaya diagnostika* (Optical Biomedical Diagnostics) (Moscow: Fizmatlit, 2007).
2. Bednov A.A., Ul'yanov S.S., Tuchin V.V., Brill' G.E., Zakharova E.I. *Izv. Vyssh. Uchebn. Zaved. Ser. Prikl. Nelin. Dinam.*, **4** (6), 45 (1996).
3. Priezzhev A.V. in *Munich European Biomedical Optics, Short Course 101* (Bellingham, WA: SPIE Optical Engineering Press, 2001).
4. Sidorov V.V., Ronkin M.A., Maksimenko I.M., Shcherbanina V.Yu., Ukolov I.A. *Biomed. Tekhnol. Radioelektron.*, **12**, 26 (2003).
5. Krupatkin A.I., Sidorov V.V. *Lazernaya Doplerovskaya floumetriya mikrotsirkulyatsii krovi* (Laser Doppler Flowmetry of Blood Microcirculation) (Moscow: Meditsina, 2005).
6. Kupriyanov V.V., Karaganov Ya.L., Kozlov V.I. *Mikrotsirkulyarnoe ruslo* (Microcirculatory Bed) (Moscow: Meditsina, 1975).
7. Chernukh A.M., Aleksandrov P.N., Alexeev O.V. *Mikrotsirkulyatsiya* (Microcirculation) (Moscow: Meditsina, 1984).
8. Levtov V.A., Regirer S.A., Shadrina N.Kh. *Reologiya krovi* (Rheology of Blood) (Moscow: Meditsina, 1982).
9. Mchedlishvili G.I. *Mikrotsirkulyatsiya* (Microcirculation) (Tbilisi: Izd. AN GSSR, 1958).
10. Shoshenko K.A. *Krovenosnye kapillyary* (Blood Capillaries) (Novosibirsk: Nauka, 1975).
11. Mchedlishvili G.I. *Mikrotsirkulyatsiya: Obshchie zakonomernosti regulirovaniya i narushenii* (Microcirculation: General Properties of Regulation and Disorders) (Leningrad: Nauka, 1989).
12. Kozlov V.I. *Dvizhenie krovi po mikrososudam i transkapillyarnyi obmen* (The Movement of Blood Through Microvessels and Transcapillary Exchange) (Leningrad: Nauka, 1984).
13. Rossini A.A., Chick W.L. in *Microcirculation* (Baltimore: University Park Press, 1980) Vol. III, p. 245.
14. Davis E. in *Microcirculation* (Baltimore: University Park Press, 1980) Vol. III, p. 223.
15. Coleridge-Smith P.D., et al. *Brit. Med. J.* **296**, 1726 (1988).
16. Hebert P.C., Qun Hu L., Biro G.P. *Can. Med. Assoc. J.*, **156**, S27 (1997).
17. Fagrell B. *Ann. Biomed. Eng.*, **14**, 163 (1986).
18. Metz S., et al. *J. Nucl. Med.*, **51**, 1691 (2010).
19. Manning W.J., Li W., Edelman R.R. *New Engl. J. Med.*, **328**, 828 (1993).
20. Rajadhyaksha M., et al. *J. Invest. Dermatol.*, **104**, 946 (1995).
21. Bonesi M., et al. *Laser Phys.*, **20**, 891 (2010).
22. Bonesi M., et al. *Laser Phys.*, **20**, 1491 (2010).
23. Gurfinkel Y.I. *Proc. SPIE Int. Soc. Opt. Eng.*, **4241**, 467 (2001).
24. Kuznetsov Yu.L., Kalchenko V.V., Meglinski I.V. *Kvantovaya Elektron.*, **41** (4), 308 (2011) [*Quantum Electron.*, **41** (4), 308 (2011)].
25. Kalchenko V., et al. *J. Biophoton.*, **4**, 645 (2011).
26. Kalchenko V., et al. *Laser Phys. Lett.*, **7**, 603 (2010).
27. Briers J.D. *Physiol. Meas.*, **22**, R35 (2001).
28. Briers J.D., Richards G., He X.W. *J. Biomed. Opt.*, **4**, 164 (1999).
29. Kalchenko V., Brill A., Bayewitch M., Fine I., Zharov V., Galanzha E., Tuchin V. *J. Biomed. Opt.*, **12**, 052002 (2007).
30. Serov A., Steinacher B., Lasser T. *Opt. Express*, **13**, 3681 (2005).
31. Meglinski I.V., Boas D.A., Yodh A.G., Chance B., Tuchin V.V. *Izv. Vyssh. Uchebn. Zaved. Ser. Prikl. Nelin. Dinam.*, **4**, 65 (1996).
32. Korolevich A.N., Meglinski I.V. *Bioelectrochemistry*, **52**, 223 (2000).
33. Meglinski I.V., Korolevich A.N., Tuchin V.V. *Crit. Rev. Biomed. Eng.*, **29**, 535 (2001).
34. Meglinski I., Tuchin V.V., in *Coherent-Domain Optical Methods for Biomedical Diagnostics, Environmental and Material Science*. Ed. by V.V. Tuchin (New York: Kluwer Acad./Plenum Publ., 2012) p. 149.
35. Snabre P., Dufaux J., Brunel L., in *Waves and Imaging through Complex Media* (New York: Kluwer Acad. Publ., 2001, p. 369).
36. Boas D.A., Dunn A.K. *J. Biomed. Opt.*, **15**, 011109 (2010).
37. Kwon S., Sevick-Muraca E.M. *Lymphat. Res. Biol.*, **5**, 219 (2007).